UN
82
S139a
1995

Applications of a Diode-laser-based Detector to On-line Determinations Involving Methylene Blue

By

Michelle Ann Spaziani

****

Submitted in partial fulfillment

of the requirements for

Honors in the Department of Chemistry

UNION COLLEGE

June, 1995

ABSTRACT

SPAZIANI, MICHELLE ANN Applications of a Diode-laser-based Detector to On-line Determinations Involving Methylene Blue. Department of Chemistry, June 1995.

The application of an inexpensive diode-laser-based detector for flow injection analysis (FIA), and the on-line determination of sulfide using the "Methylene Blue (MB) Method" [1] is presented. The detector is designed for simultaneous measurements of transmittance and fluorescence. A 670-nm diode laser is the excitation source; photodiodes serve as detector elements. The flow cell is constructed of a piece of square-cross-section quartz capillary tubing.

The MB Method employs *N,N*-dimethyl-*p*-phenylenediamine (DMPD), iron III, and sodium sulfide reacting to form MB; a triple-line flow-injection manifold is used. Performed previously using conventional UV-Vis instrumentation [1], optimized conditions included one reagent dissolved in 9 M sulfuric acid, which renders the method impractical for routine analysis. A fluorescence-based detector is more sensitive than an absorbance-based one, hence this on-line reaction can be performed under less corrosive conditions using fluorescence. Currently, our limit of detection (LOD) is 5.3×10^{-7} M injected sulfide when using 0.100 M H_2SO_4. The fluorescence response to sulfide is unaffected when using a simulated wastewater matrix; our LODs using a DMPD CS in 2.00 M and 0.100 M H_2SO_4 are 1.9×10^{-6} M and 9.7×10^{-6} M injected sulfide, respectively. The speed, simplicity, sensitive LOD, and less corrosive conditions make this method more favorable for routine analysis.

[1] Kuban, V.; Dasgupta, P.K.; Marx, J.N.; *Anal. Chem.* **1992**, *64*, 36-43

For Mom, Dad, and Michael

Acknowledgments

"It seems to me shallow and arrogant for any man in these times to claim he is completely self-made, that he owes all his success to his own unaided efforts. Many hands and hearts and minds generally contribute to anyone's notable achievements." Walt Disney

I am indebted to all Chemistry Department faculty for their time, energy, patience, words of encouragement, and praise. Their attention both in and out of the classroom are worthy of sincere thanks. More specifically, I wish to acknowledge those individuals I was fortunate enough to have as educators: Professors J.S. Anderson, M.K. Carroll, K. DeJesus, D. Hayes, L.A. Hull, K. Lou, C. Weick, and M. Yin. Professor T.C. Werner requires a special thank you for his advice, for his assistance, and for always directing unusual opportunities my way. I would also like to thank the Chemistry Department for the unlimited use of its analytical instrumentation, and the Union College Machine and Electronics Shops for their assistance and many contributions to this project.

Many thanks to the Union College Internal Education Fund (IEF) for its generous support in the form of two undergraduate research grants, the PEW Science Foundation for 1994 summer research financial support, and the Union College Chemistry Department for financial support necessary to attend the 1995 Pittsburgh Conference. Furthermore, I gratefully acknowledge the American Chemical Society Women Chemists Committee, in conjunction with Eli Lilly and Company, for awarding me a 1995 Eli Lilly and Company Travel Award for Woman Students.

I wish to thank General Electric Corporate Research and Development and the New York State Forensics Laboratory for granting me the opportunity to perform research; from these internships I have benefited greatly. A special thank you to Prof. C. Scaife for suggesting the Forensics Laboratory for independent study.

I extend a heartfelt thank you to Dr. Mary K. Carroll, my research and graduate school advisor, professor, and mentor. Thank you for directing me towards the right path while always granting me the freedom to experiment,

and for always seeing my potential, especially during those times when it was so unclear to me.

A huge thanks to Vicki Lowery and Melissa Morris for being such great lab partners. I would also like to thank my friends for their support, and for not giving up on me.

Lastly, but no less important, I wish to express my gratitude to my mom, dad, and brother for their endless love, praise, and emotional support. You made it all possible.

Michelle Ann Spaziani

Michelle Ann Spaziani

Contents

Abstract, ii

Dedication, iii

Acknowledgments, iv

Figures, viii

Tables, xi

Chapter 1 Introduction, 1

Part 1: Flow Injection Analysis, 2
Background, 3
Dispersion, 5
Tortuosity and Confluence, 9
Construction and Components of an FI Apparatus, 9

Part 2: Laser Spectroscopy, 11
Diode Lasers, 16
Miniature Instrumentation, 17
Photodiode Detectors, 17

Part 3: Methylene Blue Chloride, 18
Structure and Properties, 18
Applications of Methylene Blue, 21
The "Methylene Blue Method," 25

Literature Cited, 29

Chapter 2 **Experimental Conditions, 31**

Materials and Chemicals Employed in the Characterization of the Flow Injection System, 32
Materials and Chemicals for the "Methylene Blue Method," 32
Simulated Wastewater, 33
Flow Injection Materials, 33
Conventional Instrumentation, 35

Literature Cited, 39

Chapter 3 **Experimental Procedures and Results, 40**

Part 1: Characterization of the Triple-Line FI Manifold, 41
Injection Loop Volume, 41
Flow Rate Determination, 41
Dispersion, 42

Part 2: The MB Method with Conventional Detection, 43
Using UV-Vis Detection to View Reaction Advancement with Time, 43
Acidity Effects on MB, 43
Acidity Effects on DMPD, 48

Part 3: The Diode-Laser-Based Detector with the MB Method, 55
Fluorescence 'Dips' in Response to MB, 55
Laser Light Scatter, 55
System Reproducibility and Its Response to Sulfide Injections of Varying Concentration, 55
The Linear Relationship between Fluorescence Response and Injected Sulfide Concentration, 57
Limits of Detection, 63
The Response to Sulfide in a Simulated Wastewater Matrix, 64

Literature Cited, 70

Chapter 4 **Discussion, 71**

Literature Cited, 81

Chapter 5 **Future Research, 82**

Literature Cited, 84

Figures

1. Differences between an air-segmented stream and a nonsegmented stream in an FIA system, 4
2. Effects of convection and diffusion on the concentration profile of an analyte at the detector, 6
3. A typical FI peak profile, 8
4. Schematic diagram of an FI single-line manifold, 10
5. Diagram showing one channel of a peristaltic pump, 12
6. Schematic diagram of an FI triple-line manifold, 13
7. Energy level diagram of absorbance and fluorescence, 15
8. Diagram of a p-n junction, 19
9. Methylene blue chloride, 20
10. Acid-base behavior of Methylene blue in 0.100 M, 2.0 M, and 9.0 M sulfuric acid solutions, 22
11. Absorption spectrum of 1×10^{-6} M Methylene blue in 0.00100 M HCl, 23
12. Fluorescence spectrum of 1×10^{-6} M Methylene blue in 0.00100 M HCl, 24
13. *N,N*-dimethyl-*p*-phenylenediamine (DMPD), 26
14. The "MB Method" mechanism developed by Boltz and Howell, 27
15. The Kuban et al. proposed mechanism for the "Methylene Blue Method," 28
16. Triple-line FI manifold used for the MB Method, 34
17. Detector, 36
18. Block diagram of the virtual instrument panel for LabVIEW 2 data acquisition, 37

19. Absorbance of synthesized MB at 0 min after injecting a sulfide stock (10 mg/100 mL) solution, 44

20. Absorbance of synthesized MB at 10 minutes after injecting a 10 mg/100 mL sulfide stock solution, 45

21. Absorbance of synthesized MB at 20 minutes after injection of a 10 mg/100 mL sulfide stock solution, 46

22. Absorbance of synthesized MB at 90 min after injecting a 10 mg/100 mL sulfide stock solution, 47

23. Fluorescence spectrum of MB in 2.00 H_2SO_4, 49

24. Fluorescence spectrum of MB in 0.100 M H_2SO_4, 50

25. The absorption spectrum of DMPD in 0.100 M H_2SO_4, 51

26. The absorption spectrum of DMPD in 2.00 M H_2SO_4, 52

27. The fluorescence spectrum of DMPD in 2.00 M H_2SO_4, 53

28. The fluorescence spectrum of DMPD in 0.100 M H_2SO_4, 54

29. Reproducible fluorescence behavior in response to four sodium sulfide injections (112 mg/L) using DMPD in 2.00 M H_2SO_4, 56

30. Fluorescence of on-line MB formation from sulfide injections of varying concentration using DMPD in 9.0 M H_2SO_4, 58

31. Fluorescence response to sulfide injections of varying concentration in a DMPD solution containing 9.0 M H_2SO_4, 59

32. Fluorescence response to sulfide injections of varying concentration in a DMPD solution containing 4.5 M H_2SO_4, 60

33. Fluorescence response to sulfide injections of varying concentration in a DMPD solution containing 2.00 M H_2SO_4, 61

34. Fluorescence response to sulfide injections of varying concentration in a DMPD solution containing 0.100 M H_2SO_4, 62

35. Reproducible fluorescence behavior to replicate injections of a 62 mg/L sulfide solution, which is in simulated wastewater, into C1, 66

36. Reproducible fluorescence peaks in response to sulfide injections (56 mg/L) without wastewater, 67

37. The on-line fluorescence response to varying concentrations of sulfide prepared in an artificial matrix. The DMPD CS contains 2.00 M H_2SO_4, 68

38. The on-line fluorescence response to varying concentrations of sulfide prepared in an artificial matrix. The DMPD CS contains 0.100 M H_2SO_4, 69

39. Absorption spectrum of 0.01 μM MB in water, 78

Tables

I. Limits of detection (LODs) for sulfide, with or without a wastewater matrix, employing various concentrations of H_2SO_4 in the DMPD CS, 63

II. Average height of the fluorescence signal when using an approximate 30 mg/L suilfide solution either in water or a simulated wastewater matrix, 65

III. Calculated concentrations by LLS of injected sulfide solutions in a simulated wastewater matrix, 76

Chapter 1

Introduction

This chapter is intended to be an introduction to the three primary areas encountered in the research currently underway. In Part 1, flow injection analysis (FIA) principles, techniques, and the construction and components of an flow injection (FI) apparatus are discussed. Part 2 reports the uses of lasers in spectroscopy, and specifically describes the diode laser, which is used in this research. The miniature instrumentation utilized for experimentation is also described. Finally, Part 3 introduces Methylene blue (MB) and its biological and chemical uses. In addition, the system of research, the "Methylene Blue Method," [1,2] is explained.

PART 1: FLOW INJECTION ANALYSIS

FIA is an automatic analytical continuous-flow method [3] currently of significant use for routine biological [4], chemical [1, 5-8], and environmental [1,5-9] analyses, as well as research and development projects. Overall, FI has become a routine technique; it provides a convenient means of sample handling and treatment in the laboratory and for on-line "titrations" [10], and is of great advantage for its sensitivity, rapid sample rate (typically 10-120 s), precision, highly reproducible timing sequences, and low cost. Its low reagent consumption (typical flow rates are 0.5-2.0 mL/min) and high sample throughput also render this technique advantageous [9]. In the current research, FIA has been employed for absorbance and fluorescence measurements using

commercially available UV-Vis and fluorescence instruments, and diode-laser-based detection.

Background. Put simply, FIA is based on the injection of a liquid sample into a moving, unsegmented continuous carrier stream (CS) [11]. Mixing between the carrier and injected sample is always incomplete, yet due to the reproducibility of the mixing pattern, FIA yields results with high precision [11]. What happens to one sample, happens in the same manner to any other. The injected sample forms a zone, which is transported through a flow cell toward a detector. The detector measures the physical parameter of interest as it continuously changes while passing through the flow cell [11]. A variety of detectors are used in FIA; common parameters include absorbance (transmission), fluorescence, scattering, and electrode potential.

In FI methods first described in the 1970's by Ruzicka and Hansen [1,12], closely spaced air bubbles (an air-segmented system) were thought to be useful for several purposes [3]: to prevent excess sample dispersion (band broadening), promote turbulent mixing of samples and reagents, and scrub the walls of the conduit, hence preventing cross-contamination between samples. In reality, air bubbles pose a problem; separation of the liquid segments occurs when air bubbles exist [11] {Figure 1}. The liquid mixes within individual segments, causing a homogeneous mixture at the detector and a steady-state signal [11]. The transition from the baseline to the steady-state height level requires several washings, hence a large sample volume aspirated into the system. The steady-state height is then relatively independent of physical and chemical kinetics of the system. In nonsegmented systems, this problem is alleviated due to production of a stratified liquid at the detector [12]. In addition, nonsegmented

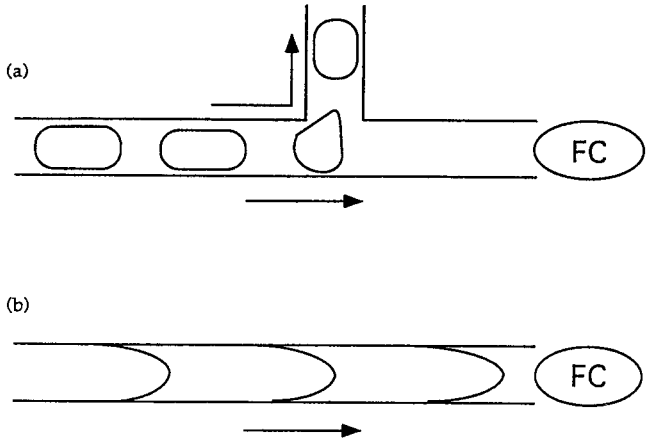

Figure 1. Differences between the air-segmented stream (a) and the nonsegmented stream (b) in an FIA system. Air bubbles separate the liquid in the former; mixing occurs between the segments resulting in a homogeneous stream at the flow cell (FC). To prevent disturbed signals at the detector, the air segmentation is removed in a debubbler via differential pumping (the flow rate of the solutions entering the debubbler is larger than the flow rate drawn through the FC). In the non-segmented stream, the liquid is stratified [11].

systems yield much higher sampling frequency than segmented streams.

It was found that cross-contamination and excess dispersion could be avoided, and thorough mixing of samples and reagents could then be accomplished, in a nonsegmented system [3]. Important advantages to systems free of air bubbles [3] include 1.) higher analysis rates, 2.) enhanced response times, 3.) rapid start-up and shut-down times, and 4.) simpler and more flexible equipment, except for the injection port. Most important, however, is controlling dispersion of the sample zone [11].

Dispersion. A typical FI peak resembles that of a poorly resolved chromatographic peak, where the peak height and width are directly proportional to the analyte concentration. Ruzicka and Hansen [11,12] found that the sample zone disperses according to convection, or the parabolic velocity profile characteristic for laminar flow, where the liquid in the center of the tube moves at twice the mean speed of the fluid; the layers closer to the wall are increasingly more retarded with time {Figure 2 (b)}. The sample zone follows movement of the CS, forming a dispersed zone whose form depends on the geometry of the tubing and flow velocity.

Broadening also occurs as a result of diffusion [3]. As depicted in Figure 2 (d), molecules of the sample on the leading boundary diffuse towards the walls and enter the slower moving streams; by contrast, molecules on the trailing boundary diffuse towards the middle of the tube and enter faster moving stream lines [13]. The effect of diffusion is to slow down the front boundary while speeding up the rear [13].

Two types of diffusion are possible: radial (perpendicular to the flow direction), and longitudinal (parallel to the flow) [3]. At low pump speeds, the

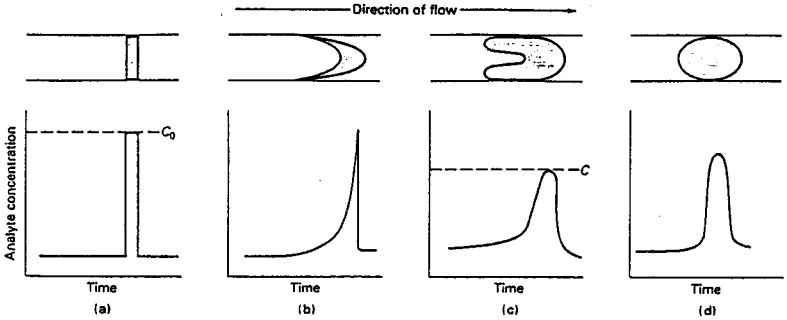

Figure 2. Effects of convection and diffusion on concentration profiles of analytes at the detector. No dispersion is illustrated in (a), dispersion by convection, (b), dispersion by convection and radial diffusion, (c), and dispersion by diffusion, (d). Reprinted from [3].

former is often the major source of dispersion in narrow tubing. However, longitudinal diffusion is of no significance in narrow tubing at any pump speed [3]. FIA is usually performed under the conditions in which dispersion occurs via convection and radial diffusion [3] {see Figure 2 (c)}. Cross-contamination is limited or eliminated with these conditions.

Knowledge of how to control dispersion is vital in understanding how FIA works. It is imperative to know [12] 1.) how much the original sample solution is diluted before reaching the detector, and 2.) how much time elapses between sample injection and the readout. The dispersion coefficient (D) is defined [3] by the equation

$$D = C^{o}/C_{p}$$

where C^{o} is the analyte concentration of the injected sample and C_p is the peak concentration {Figure 3}. It is the single most important variable that is able to describe the type of system constructed. The method commonly used to measure D is to inject a dye solution of known C^{o} into a colorless CS. Absorbance is measured in the flow cell, and after calibration, C is calculated from Beer's Law

$$A = \varepsilon bC$$

where A is absorbance, ε is molar absorptivity in L $mol^{-1}cm^{-1}$, b is cell path length in cm, and C is concentration in mol L^{-1} [3].

The D value, normally used to characterize the extent of mixing in a particular FI system, is classified as *limited* (1 to 3), *medium* (3-10), and *large* (>10) [3]. Generally speaking, when D = 2, the sample solution has been diluted

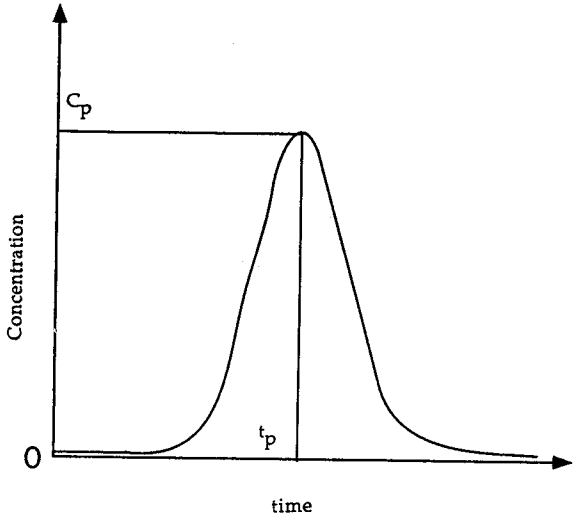

Figure 3. A typical FI peak profile. C_p is the concentration of analyte at the peak maximum; t_p is the time expired after injection of the analyte.

1:1 with the CS [11]. Controllable variables including injected sample volume, tube length, and pump speed influence D. Tyson [13] summarizes Ruzicka and Hansen's findings, reporting that D increases with increasing 1.) tube length, 2.) tube diameter, 3.) increasing average flow rate, and 4.) detector volume; D decreases with increasing sample volume and increasing tortuosity of tubing. Note that at large sample volumes, D becomes unity and no significant mixing of CS and sample takes place [3]. Only with experience and changing parameters can one assemble a reaction zone with a desired D value.

Tortuosity and Confluence. The confluence of merging streams [13] exists as a second mechanism (the first being inter-diffusion of the sample and reagent) by which to mix the sample and CS. In addition, production of secondary flow patterns to aid mixing is accomplished by FIA microreactors, or channel geometries. These include coiled or knitted tubing, and mixing chambers. The function of these microreactors is to increase the intensity of the radial mixing and reduce the parabolic velocity profile in the axial direction (formed when the sample zone is injected into a laminar flow of CS). As a result, the reagent becomes more readily mixed with the sample, and the axial dispersion of the sample zone is reduced.

Construction and Components of an FI Apparatus. An FI apparatus can be simple or elaborate depending on the on-line reaction of interest. The simplest system, a single-line manifold, consists of only a variable speed peristaltic pump (P), an injection valve (V), an injection port for sample introduction (I), manifold components (a mixing coil, MC), a detector (d), and a recorder or computer (Figure 4).

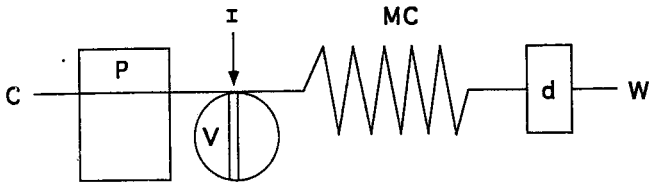

Figure 4. Schematic diagram of an FI single-line manifold. C, carrier stream; P, peristaltic pump; V, injection valve; I, port for sample introduction; MC, mixing coil; d, detector; W, waste. A computer or recorder is used at d.

The pump device is used to squeeze fluid through plastic tubing by rollers, forcing a continuous, relatively pulse-free, flow of fluid [3] (Figure 5). Its advantages [13] include availability of several channels of variable flow, availability of a variety of pump tube materials, and precise control over on/off periods.

A low pressure six-port or eight-port rotary injection valve is often used. Injection volumes range from 5 to 2000 μL [3] and are injected quickly as a pulse of liquid by manually turning the injection valve 90°. These injections are referred to as slugs of liquid [13]. Greater dispersion in the rear boundary results; the manifold is longer for this boundary than for the leading boundary by the length of the injection loop [13].

Manifold components are normally comprised of low pressure chromatography fittings with narrow-bore Teflon® poly(tetrafluoroethylene) (PTFE) tubing of 0.5 or 0.8 mm internal diameter (i.d.) [13]. As described in the previous section, the tubing is coiled or contorted to promote thorough mixing.

The complex triple-line manifold designed for this research is shown in Figure 6. The analytical scheme of interest requires several reagent solutions, which are mixed before and/or after sample introduction. This manifold consists of three CSs in which the reagents flow separately until a desired confluence point is reached; eventually, the sample is injected into one CS, then carried through to the flow cell and detector.

PART 2: LASER SPECTROSCOPY

Prior to the development of the laser (light amplification by stimulated emission of radiation) in the 1960's, the primary source of optical radiation [14]

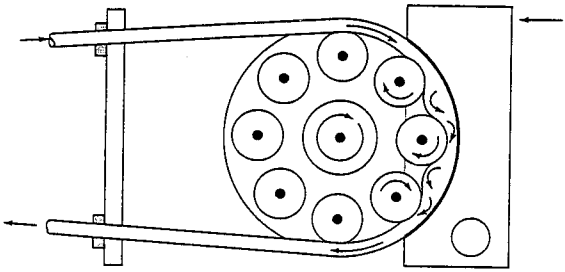

Figure 5. Diagram showing one channel of a peristaltic pump. In the current research, there are three pieces of pump tubing placed adjacent to each other on top of the rollers. Reprinted from [3].

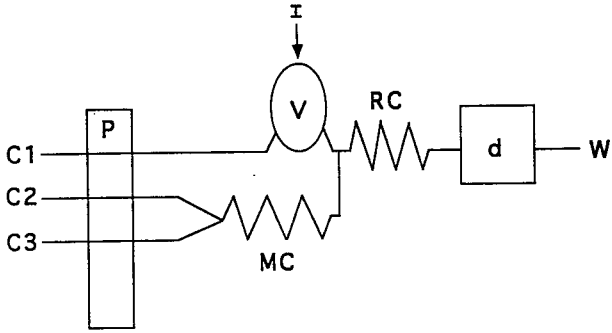

Figure 6. Schematic diagram of an FI triple-line manifold. P, peristaltic pump; V, injection valve; I, sample introduction; MC, 200 x 0.5 mm mixing coil; RC, 2000 x 0.5 mm reaction coil; d, detector; W, waste. C represents a carrier stream, where C1 is 25.0 mM NaOH, C2 is 16 mM $FeNH_4(SO_4)_2$ in 0.100 M H_2SO_4, and C3 is 2 g/L DMPD in 9.0 M H_2SO_4. C2 and C3 flow at the same rate; C1 flows at twice that of C2 and C3.

in chemical instrumentation was the lamp; for commercial instruments, this is still true. Lamps provide stable and sufficient output power for easy detection and measurement in spectroscopic studies. However, great disadvantages [14] including incoherent emission and tuning incapability became evident. The laser was developed to compensate for these problems.

Lasers have presented several advantages such as beam-focusing capability, near-monochromaticity, ultrahigh sensitivity, selectivity, and large photon flux [15]. In general, a laser's ability to focus down to a small area provides excellent spatial resolution [3] (resolution produced via data obtained simultaneously from different regions of the spectrum) , and its monochromaticity allows for high spectral resolution. Most important, however, is the large photon flux (energy); it is the key to the success of the laser. The higher the photon flux at a given point, the more photons available for the species to absorb. In measuring absorbance (the amount of energy *absorbed* by the molecule as it is promoted to the excited state), this strong light source leads to more beam light reaching the detector, and allows for measurements of species of low concentration. However, this large light throughput renders measurement of a small absolute change in signal very difficult. Laser fluorometry is utilized in this research; it is the study of the *emitted* radiation from a radiational transition between states with the same spin quantum number, e.g. $S_1 \rightarrow S_0$, after exposure to light. For fluorescence measurements, increased emission results because fluorescence is proportional to incident light. Ultra-high sensitivity results due to the large photon flux. Figure 7 presents a energy level diagram of absorbance and fluorescence.

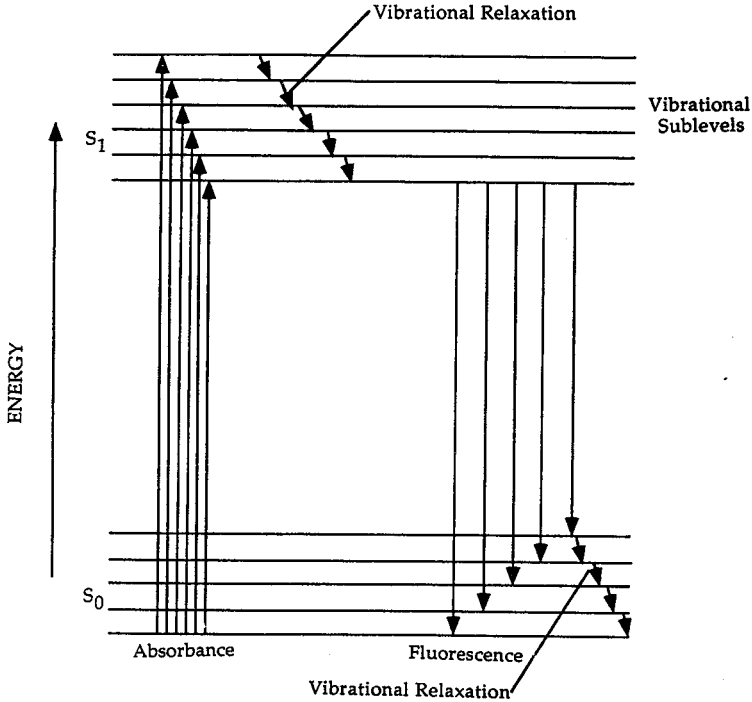

Figure 7. Energy level diagram of absorbance and fluorescence. S_0 is the ground singlet state, and S_1 is the lowest excited singlet state.

Diode Lasers. Diode lasers [16] are small, reliable, relatively inexpensive, solid-state, semiconductor-based devices that have several of the advantages of the more conventional lasers. They are simpler in that they are free of internal optical elements [17]. In addition, the inherent low noise and narrow spectral linewidth make these lasers unique. The diode laser's characteristic of tunability, accomplished by altering the laser's temperature or the strength of a magnetic field, also renders it advantageous [14]. The trend of increasing usage and technology of the diode laser continues as its 'good and reliable' reputation gains recognition in the scientific community.

Put simply, diode lasers can be viewed as light emitting diodes (LEDs) with mirrored sides [18], which produce a stable and well-focused beam of light. LEDs are not lasers; their output is spontaneous emission, similar to that of a light bulb where light is emitted in all directions [19]. Lasers, on the other hand, produce outputs of stimulated emission. Excited particles of the laser medium are struck by photons having the same energy as those produced by spontaneous emission [3]. As a result, a photon is emitted with the same energy as that which stimulated the process. The emitted proton and the photon that caused emission travel in the same direction and in the same phase. Stimulated emission, therefore, is coherent with the incoming radiation. A feedback loop maintains constant optical output power for this operation. In this study, the total output power is approximately 3 mW for a 635 nm laser diode, and 8 mW for a 670 nm.

Two types of diode lasers [17] are available: visible and near-infrared lasers fabricated from the group III-V semiconductor compounds, and the lead-salt lasers, which operate at wavelengths 3 and 30 μm. The former are applied in the current research.

The majority of semiconductor-based diode lasers available emit in the red and near-infrared regions [16], yet development towards increased output power at shorter emission wavelengths is underway. Presently, we are limited to certain lasers emitting in these regions, yet this has one great advantage; few species absorb or fluoresce in the red or near-infrared, hence chemical interferences are not encountered frequently. We have used a 670-nm diode laser in the miniature instrumentation constructed by a former undergraduate student [20]. The species of interest exhibits an absorption maximum (664 nm) which almost exactly coincides with the 670-nm semiconductor laser.

Miniature Instrumentation. The miniature instrumentation utilized was developed by James L. Davis as part of his Senior research project [20]. The detection circuitry in the instrument was developed by Marc A. Unger [18]. The instrument is small, relatively inexpensive, reliable, and solid-state, capable of detecting transmittance, fluorescence, and scattered light simultaneously. Unger states that "by means of lenses, (and) filters..., we select the signal that we want - absorbance fluorescence, or scattering - and separate it form the unwanted signals" [18]. The optical signal is then transduced into an electric signal, the incident light produces a current of electrons, and the electrical circuit amplifies the signal, removing the noise. Lastly, the data is produced via computer hardware and software.

The design of the laser module, sample holder, and electronics are described in great detail in Unger's thesis [18].

Photodiode Detectors. Photodiode detectors are sensitive, solid-state sensors constructed to detect the intensity of light. They are favored for their

rapid response, wide linear range of transmitted light, and small size. The latter allows for the possibility of miniature instrumentation.

Photodiode detectors make use of the photovoltaic effect, the generation of a voltage across a p-n (positive and negative) junction of a semiconductor when the junction is exposed to a light source [21]. Illustrated in Figure 8, the p-n junction consists of side-by side p- and n-regions, in which a charge occurs with incident light [3]. When light strikes a photodiode, the electrons within its structure are stimulated, resulting in electron-hole pairs as electrons are pulled from their conduction band. This results in a p-region and a n-region. The p-region consists of mobile holes and stationary positive ions; the n- region, with mobile electrons and stationary negative ions. The photodiode itself absorbs photons at the p-n junction to produce a current proportional to the incident radiation, i.e. the signal from the photodiode is linear to the amount of applied light power [3].

Photodiodes exhibit 1) excellent linearity, 2) low noise, 3) wide spectral responses, 4) long lifetimes, and 5) high sensitivity [19]. In addition, they are compact, lightweight and relatively inexpensive, costing approximately $3 each.

PART 3: METHYLENE BLUE CHLORIDE

Structure and Properties. Methylene blue chloride (MB) is a basic, organic dye that absorbs, and subsequently, fluoresces in the deep-red spectral region (~670 nm); it is used extensively with diode lasers emitting primarily in this region {Figure 9}. MB, a dark green odorless crystal with bronze luster or crystalline powder, is extremely soluble in water; however, in a similar

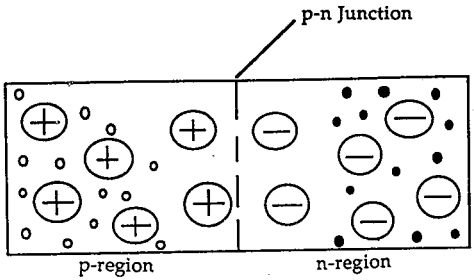

Figure 8. Diagram of a p-n junction. The electrons (colored in) are attracted to a region of positive charge, and the holes (open circles) are attracted to a region of negative charge.

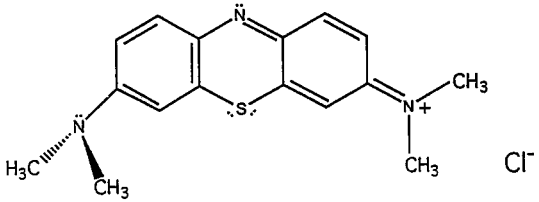

Figure 9. Methylene blue chloride.

fashion to other polymethine dyes, MB photodegrades when in an aqueous solution [22]. Preparing MB in a slightly acidic solution ameliorates this problem. Most MB solutions used in this research have been prepared in acidic solutions of either sulfuric or hydrochloric acid.

MB is an acid-base indicator. The redox reaction of MB is reversible over the pH range of 1 to 13. The colorless leuco MB (Methylene White) is light sensitive. When left open to light, but in the absence of air, the colorless solution rapidly redevelops the blue color of MB. The standard reduction potential (E^{O}) of MB is 0.532 Volts (V) [23].

At pH $\geq$ 1, MB exists as MB^{+} with a characteristic absorbance peak maximum at 664 nm. With increasing acidity, a red-shift is evident; the MBH^{2+} maximum is at 745 nm. Figure 10 illustrates the red-shift observed when sulfuric acid concentrations of 0.100, 2.0 and 9.0 M are spiked with $1x10^{-3}$ MB.

The absorbance and fluorescence spectra of $1x10^{-6}$ M Methylene blue in 0.001 M HCl are illustrated in Figures 11 and 12, respectively. Characteristic absorbance peaks are at 246 nm, 292 nm, and 664 nm with a shoulder at 612 nm. The peak at 664 nm is the maximum. A characteristic fluorescence peak in an emission spectrum results at 706 nm when excited at 246 nm. The peak at 492 is scattered light. These data have been obtained with conventional absorbance and fluorescence instrumentation.

Applications of Methylene Blue. MB is used extensively in both chemical and biological research. It is used in measurements of oxidation and reduction potential, determinations of enzymes and metabolites, and DNA

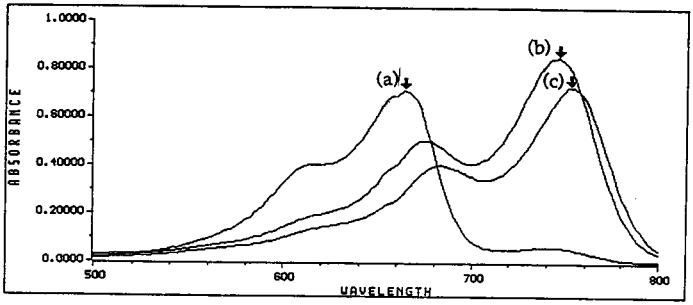

Figure 10. Acid-base behavior of Methylene blue in 0.100 M, 2.0 M, and 9.0 M sulfuric acid solutions. A red-shift is evident. Peak (a) maximum is at 654 nm and 0.712 AU. For peak (b) the maximum is at 746 nm and 0.85 AU, and for peak (c), at 752 nm and 0.73 AU.

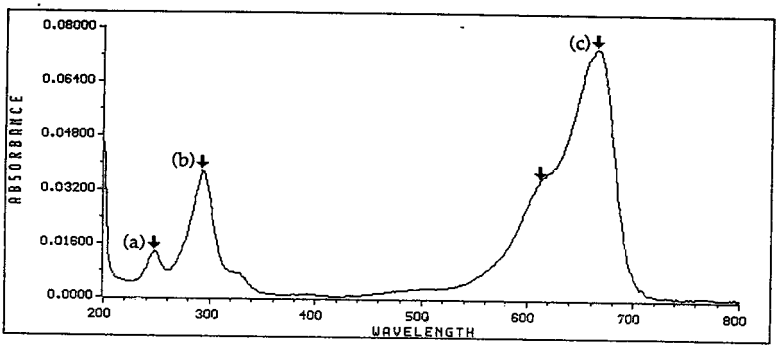

Figure 11. Absorption spectrum of 1×10^{-6} M Methylene blue in 0.00100 M HCl. Peak (a) is at 246 nm and 0.0136 AU, and peak (b) is at 292 nm and 0.0376 AU. The shoulder of the peak exhibiting maximum absorbance is at 612 nm. The absorbance maximum, (c), is 0.0747 AU at 664 nm.

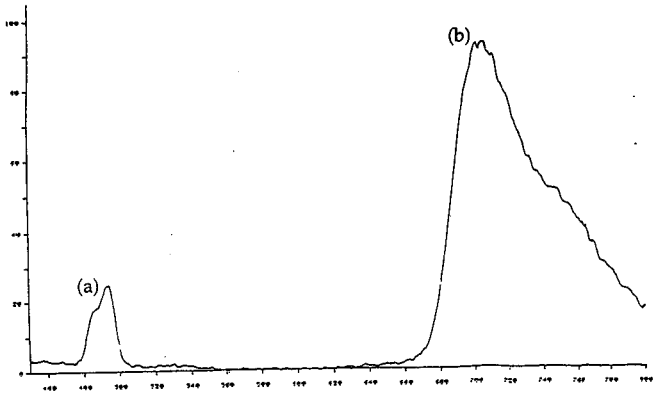

Figure 12. Fluorescence spectrum of 1.00 x 10^{-6} M Methylene blue in 0.00100 M HCl. The excitation wavelength (ex λ) is 246 nm and the slit width is 5 nm. The characteristic fluorescence peak, (b), is at 706 nm. Peak (a) at 492 nm is due to scatter.

staining [15]. In addition, MB has been employed for staining mitochondria, Negri bodies in brain tissue, elastic fibers, normal and pathological animal tissues, and connective tissue [24].

The "Methylene Blue Method". The system of interest, the "Methylene Blue Method," [1,2,24] is a well-known technique for the determination of sulfide. It depends on the formation of MB from the oxidative coupling of sulfide with *N,N*-dimethyl-*p*-phenylenediamine (DMPD), or DMPD in salt form, in the presence of iron(III). Fisher first reported sulfide's reaction to form MB in 1883 [25].

DMPD is illustrated in Figure 13. It should be noted that while the product of the MB Method is undisputed, the mechanism is far from well-known. The mechanism first suggested by Boltz and Howell is presented in Figure 14. Here, DMPD is oxidized by Fe^{3+} to form an intermediate, and then reduced by H_2S to form the phenothiazinium dye, MB [1,25]. A more recent and elaborate proposed mechanism of this reaction, represented by Kuban et al., involves an overall 6-electron oxidation of a 1,4-diaminobenzene nucleus three separate times [1] {Figure 15}.

Because a fluorescence-based detector is more sensitive than an absorbance-based one, the determination of sulfide using the MB Method can be performed under less corrosive conditions that those reported in the literature [1] using the diode-laser-based detector with fluorescence detection. In addition, better detection limits are possible. We present performance of the reaction on-line under more practical conditions using fluorescence detection.

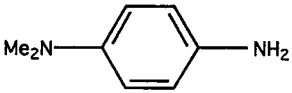

Figure 13. *N,N*-dimethyl-*p*-phenylenediamine (DMPD).

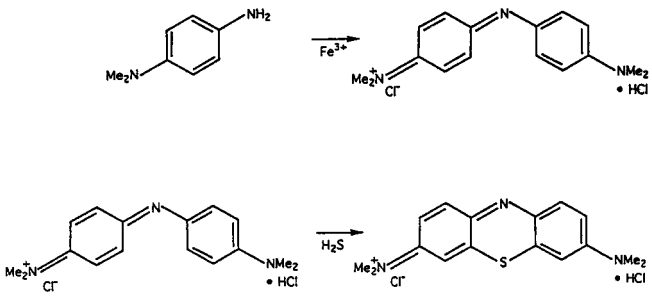

Figure 14. The "MB Method" mechanism developed by Boltz and Howell [1,24].

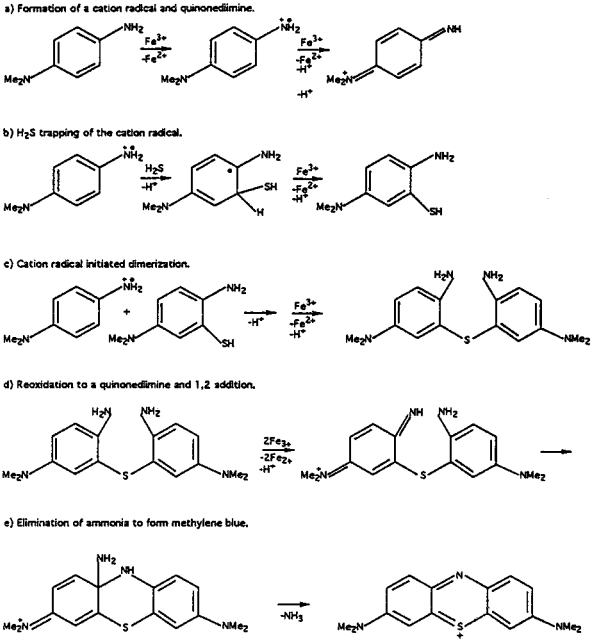

Figure 15. The Kuban et al. proposed mechanism for the "Methylene Blue Method" [1].

Literature Cited

[1] Kuban, V.; Dasgupta, P.K.; Marx, J.N.; *Anal. Chem.* **1992**, *64*, 36-43.

[2] Lei, W.; Dasgupta, P.K.; *Anal. Chim. Acta* **1989**, *226*, 165-170.

[3] Skoog, D.A.; Leary, J.J.; *Principles of Instrumental Analysis*, 4th ed.; Saunders College: Forth Worth, TX, 1992; 682-690.

[4] Abdalla, M.A.; Fogg, A.G.; Baber, J.G.; Burgess, C.; *Analyst* **1983**, *108*, 53-57.

[5] del Valle, M.; Alonso, J.; Bartroli, J.; Marti, I.; *Analyst* **1988**, *113*, 1677-1681.

[6] Sanz-Martinez, A.; Rios, A.; Varcarcel. M.; *Anal. Chim. Acta* **1993**, *284*, 189-193.

[7] DeSalvo, D.P.; Street, K.W., Jr.; *Analyst* **1986**, *111*, 1307-1310.

[8] Rios, A.; Luque de Castro, M.D.; Varcarcel, M.; *Analyst* **1984**, *109*, 1487-1492.

[9] Andrew, K.N.; Blundell, N.J.; Price, D.; Worsfold, P.J.; *Anal. Chem.* **1994**, *66*, 916A-922A.

[10] Trojanowicz, M.; Worsfold, P.J.; Clinch, J.R.; *Trends Anal. Chem.* **1988**, *7*, 301-305.

[11] Ruzicka, J.; Hansen, E.H.; *Flow Injection Analysis;* Wiley: New York, 1981.

[12] Ruzicka, J.; Hansen, E.H.; *Flow Injection Analysis*, 2nd ed.; Wiley: New York, 1988.

[13] Tyson, J.; *Basic Principles of Flow Injection Analysis*, Presented at the Flow Injection-Atomic Spectroscopy Short Course, University of Massachusetts, Amherst, MA, 1992, 1-9.

[14] Camparo, J.C.; *Contemp. Phys.* **1985**, *26*, 443-477.

[15] Imasaka, T.; Ishibashi, N.; *Anal. Chem.* **1990**, *62*, 363A-371A.

[16] Imasaka, T; *Spectrochim. Acta Rev.* **1993**, *15*, 329-348.

[17] Fox, R.W.; Weimer, C.S.; Hollberg, L.; Turk, G.C.; *Spectrochim. Acta Rev.* **1993**, *15*, 291-299.

[18] Unger, Marc A.; Senior Thesis, Union College, 1993.

[19] Hecht, J.; *Understanding Lasers;* IEEE Press: New York, 1992.

[20] Davis, J.L.; Senior Thesis, Union College, 1993.

[21] Hamamatsu Consumer Catalog, *Photodiodes*, 1991

[22] Imasaka, T.; Tsukamoto, A.; Ishibashi, N.; *Anal. Chem.* **1989**, *61*, 2285-2288.

[23] Gurr, E.; *Methylene Blue;* Williams and Wilkins: Baltimore, Maryland, 1962.

[24] Boltz, D.F.; Howell, J.A.; *Colorimetric Determination of Nonmetals;* Wiley: New York, 1978.

[25] Fisher, E.; *Ber.* **1883**, *16*, 2234.

Chapter 2

Experimental Conditions

This chapter presents the experimental materials, chemicals, and equipment employed for our research; those needed for preliminary studies will not be described. All chemicals were of reagent grade, and deionized water was used throughout as solvent, except where indicated otherwise.

Materials and Chemicals Employed in the Characterization of the Flow Injection System. Methylene blue chloride (MB) was purchased from Eastman Kodak, Rochester, NY, and Aldrich, Milwaukee, WI. Phenol red indicator was bought from LaMotte Chemical, Baltimore, MD; methyl orange indicator (powder form), from Mallinckrodt, St. Louis. Standard sodium carbonate (99.89%) was purchased from Thorn Smith, Beulah, MI. Tygon pump tubing of 1.14 mm i.d. (Cole-Parmer) was used for determination of the injection loop volume.

Materials and Chemicals for the "Methylene Blue Method." The MB Method protocol was similar to that of Kuban and coworkers [1]. Hydrochloric acid (12.1 M) and sulfuric acid (18.0 M) were obtained from Fisher, Fairlawn, NJ. *N,N*-dimethyl-*p*-phenylenediamine (DMPD, Aldrich) solutions were prepared by adding 500 mg of the salt to 250 mL of 9.0 M, 4.5 M, 2.00 M, or 0.100 M H_2SO_4; the concentration of DMPD in solution was kept constant at 9.56×10^{-3} M. A 16-mM ferric ammonium sulfate (Merck, Rahway, NJ) solution was prepared in 0.10 M H_2SO_4. Stock solutions containing ~100 mg/L sulfide were prepared

daily from sodium sulfide ($Na_2S \bullet 9H_2O$, 98%, Aldrich) in an aqueous solution of 25 mM NaOH (Fisher) made with boiled deionized water. Working sulfide solutions (~6 to ~150 mg/L) were prepared by dilution of the stock immediately before use.

Simulated Wastewater. A stock solution of synthetic wastewater [1] contained 500 mg/L of each phenol, CH_3COONa, NaCl, KCl, $CaCl_2$, KSCN, and Na_2CO_3, in addition to 100 mg/L of $Na_2S_2O_3$ and 150 mg/L of $(NH_4)_2SO_4$. It was prepared in 25 mM NaOH made with boiled deionized water. If not mixed, the solution was clear and a precipitate was evident. Sulfide was added to a small volume of a thoroughly-mixed synthetic wastewater stock solution immediately before use. The sulfide solution was mixed well before injecting on-line.

Flow Injection Materials. The FI apparatus shown in Figure 16 was used in conjunction with transparent Tygon pump (0.64 inner diameter, i.d., and 0.44 i.d., Cole-Parmer) and Teflon flow tubing (0.5 i.d., Upchurch Scientific), a four-channel, variable-speed peristaltic pump (Ismatec-sa) operated at 10 rpm, a flow cell (FC) of square-cross-section quartz capillary tubing of 1.0 mm i.d. (Wale Apparatus), and an injection loop of 69.6 ± 0.9 μL controlled by a manual six-port rotary sample introduction valve (Alltech). Tygon was not recommended for use with concentrated acids [2]; however, we chose to use this polymer because of its flexibility and availability in a convenient size. Unfortunately, severe effects were noticed and the tubing had to be replaced often. Teflon (a chemically inert fluorocarbon, PTFE) flow tubing, recommended for use with organic and inorganic acids and bases [2,3], was employed. No deterioration was

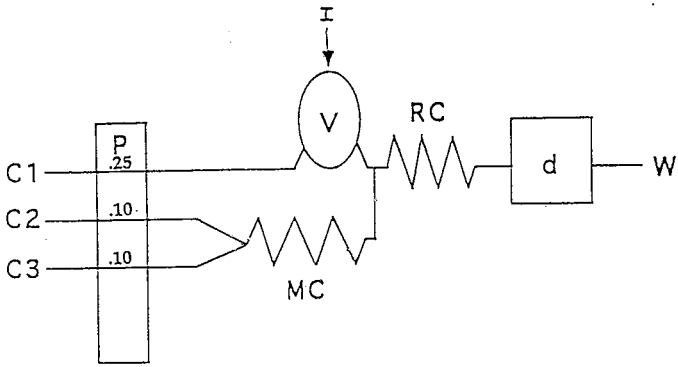

Figure 16. Triple-line FI manifold used for the MB Method. P, peristaltic pump; V, injection valve; I, sample introduction; MC, 200 x 0.5 mm mixing coil; RC, 2000 x 0.5 mm reaction coil; d, detector; W, waste. C1 is 25.0 mM NaOH, C2 is 16 mM $FeNH_4(SO_4)_2$ prepared in 0.100 M H_2SO_4, and C3 is 2 g/L DMPD in 9.0 M, 4.5 M, 2.00 M, or 0.100 M H_2SO_4. The flow rates are in mL/min.

noticed in the Teflon flow tubing. Two Omnifit three-way connectors made of PTFE (Cole-Parmer) were used in conjunction with polypropylene (PP) caps, PTFE cones, and o-rings. An flow injection analysis (FIA) adapter for peristaltic tubing was purchased from Upchurch Scientific. Flangeless fittings included Tefzel ferrules and nuts and were utilized for 1/16" outer-diameter (o.d.) tubing; the Tefzel polymer, ethylenetetrafluoroethylene, has been known to be extremely resistant to chemical attack [3]. Long FIA coilers (Upchurch) were also employed for the mixing and reaction coils, which were designed in a tight coiled fashion to promote through mixing. The dispersion coefficient (D) for this system calculated from data obtained with the diode-laser and fluorescence detection is 10.4, whereas with an absorbance-based conventional instrument, D is 8.30. The detector [4], shown in Figure 17, included a 670-nm diode-laser source (Power Technology, 8 mW) and PIN photodiode detectors (Honeywell). A Roscolux filter (Medium Blue, #83) was used to limit the amount of scattered light that reached the fluorescence photodiode. A current-to-voltage converter, assembled in house, was used at a gain setting of 10^7 [4,5]. LabVIEW 2 software was utilized for data acquisition, display, and manipulation. The block diagram of the virtual instrument for LabVIEW 2 data acquisition is shown in Figure 18.

Conventional Instrumentation. Steady-state absorbance measurements were taken using a Hewlett-Packard 8452A Diode Array Spectrophotometer with a fused-silica absorbance cell of path length 1.00 cm. In some experiments, general and kinetic scanning modes operating at wavelengths of 656 nm, 670 nm, or 748 nm were used. Steady-state fluorescence emission spectra were obtained at an excitation wavelength of 280 nm or 670 nm via a Perkin-Elmer

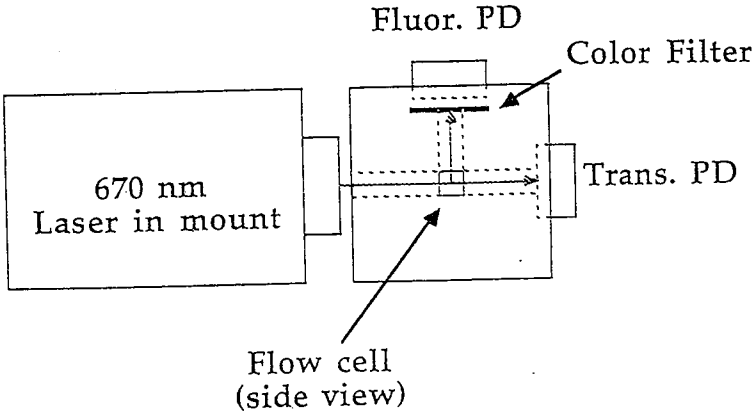

Figure 17. Detector [4]. The photodiodes (PD), which serve as detector elements, are positioned at 90° from the laser port for fluorescence detection; for transmittance, 180°. A color filter (Roscolux, Medium Blue, #83) is used to limit the amount of scattered light that reaches the fluorescence PD.

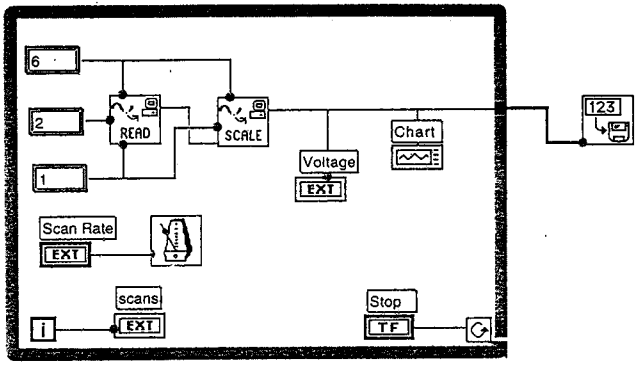

Figure 18. Block diagram of the virtual instrument panel for LabVIEW 2 data acquisition.

LS-5B Luminescence Spectrometer with a cell of path length 1.00 cm. A Hellma flow cell (stock number 176.752-QS) of path length 0.15 cm was used in both conventional instruments in kinetic studies.

Literature Cited

[1] Kuban, V.; Dasgupta, P.K.; Marx, J.N.; *Anal. Chem.* **1992**, *64*, 36-43.

[2] Cole-Parmer Instrument Catalog, 1558, 1860.

[3] Upchurch Scientific Catalog, *1993 Catalog of Chromatography and Fluid Transfer Fittings*, 28-32, 56, 60, 70.

[4] Carroll, M.K.; Davis, J.L.; Presented at the FACSS Conference, Detroit, MI, October, 1993; paper 152.

[5] Unger, M.A.; Senior Thesis, Union College, 1993.

Chapter 3

Experimental Procedures and Results

PART 1: CHARACTERIZATION OF THE TRIPLE-LINE FI MANIFOLD

Injection Loop Volume. The procedure used was acquired from a recent report [1]. First, 0.2 M HCl and 1.000 M NaOH solutions were prepared. The exact concentration of the HCl stock solution, 0.1913 M ± 0.2 ppt, was determined by conventional titration with pure, dry sodium carbonate. Methyl orange was the indicator (pH range 3.1-4.4) employed. This solution was diluted 100 fold; its molarity was recalculated at 0.001924 M after calibrating the 1000-μL pipette used for the dilution. Secondly, titration of injected 1.000 M NaOH was executed on-line using a single line manifold as seen in Figure 4. A deionized water carrier stream (CS) was used. Neither the type or size of pump tubing mattered in this case, nor did the speed at which the pump was set. Two drops of phenol red indicator (pH range 6.4-8.0) were added to the sample, which was collected in a clean, dry beaker. Finally, titration of this NaOH solution with the standard acid allowed for determination of the injection loop volume, 69.6 ± 0.9 μL (based on four replicate measurements).

Flow Rate Determination. The flow rates for the two reagent lines and the CS were determined by timing the rate at which a 10-mL volumetric flask was filled with deionized water at 10 rpm. This pump speed was chosen for one reason: we obtained a large fluorescence response to on-line methylene blue (MB) formation at this speed with a nominal effect from fluctuations in the flow

of the three lines. Using the pump at slower speeds brought about greater fluctuation, hence more noise detected by the fluorescence photodiode, and a larger dispersion coefficient (D). Using the pump at a faster speed (20 rpm) brought about a slight decrease in the fluorescence response to the MB production. D would be lower at 20 rpm and faster pump speeds.

The flow rate of the 25 mM NaOH line (Figure 16) is 0.2484491 ± 0.0000001 mL/min based on three replicate measurements. C2 is 0.10 mL/min; this determination is based solely on one measurement. C3 is assumed to be the same since C2 and C3 use pump tubing having the same i.d.

The flow rate of the FI system was determined in a similar fashion. It is 0.4494879 ± 0.0000002 mL/min, which agrees well with the anticipated value of 0.45 mL/min.

Future work may include justifying these determinations by calculating the flow rates using a simple acid-base titration technique, similar to that used in determining the injection loop volume.

Dispersion. The dispersion of the flow injection (FI) system was measured using the diode-laser-based detector and fluorescence detection, as well as with a conventional instrument for absorbance-based detection. In both cases, 1.00×10^{-5} M MB was injected in triplicate into a water CS with the reagent lines also being water. Using the diode-laser-based detector, the average peak fluorescence signal of MB at the detector is 0.261 V; the steady-state fluorescence signal of MB is 2.70 V after correcting for the background fluorescence signal. D is 10.4. Using the absorbance-based detector, the average peak absorbance signal of MB at the detector is 0.0101 AU, and the steady-state absorbance is 0.0829 AU,

and D is 8.30.

PART 2: THE MB METHOD WITH CONVENTIONAL DETECTION

Using UV-Vis Detection to View Reaction Advancement with Time. UV-Vis instrumentation was utilized in a preliminary trial to determine whether or not the MB Method worked, and if so, how this reaction progressed with time. A slug of a sulfide stock solution (10 mg/100 mL) was injected into C1 {Figure 16} on-line and the eluent was collected in a clean, dry beaker. An absorbance measurement was taken immediately. Thereafter, measurements were taken at specific time intervals; the solution was stirred occasionally. The procedure was repeated with a 50 mg/L working solution. No observable color change resulted in either case. The absorbance data, however, shows the reaction does occur with time.

As time elapsed, the reaction advanced as illustrated in the absorbance data at each time point. Figures 19, 20, 21, and 22 illustrate the increase in absorbance in the size of the peak at 748 nm, at 0 min, 10 min, 20 min, and 90 min, respectively, for injection of the sulfide stock. Results are similar for the 50 mg/L working solution. The peak at 656 nm is not due to absorbance; it is an instrumental artifact.

Acidity Effects on MB. 1 mM MB was examined in solutions of varying pH, 1 (a), -0.3 (b), and -1 (c). Measurements were made using UV-Vis detection. The acidity of the solution affects the spectral characteristics of MB. A spectral red-shift results with decreasing pH {Figure 10}. The fluorescence (in relative

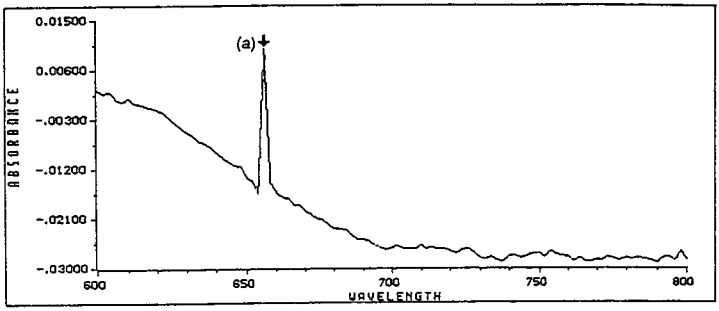

Figure 19. Absorbance of synthesized MB at 0 minutes after injecting a sulfide stock (10 mg/100 mL) solution. Peak (a) at 656 nm is not due to absorbance; it is an instrumental artifact.

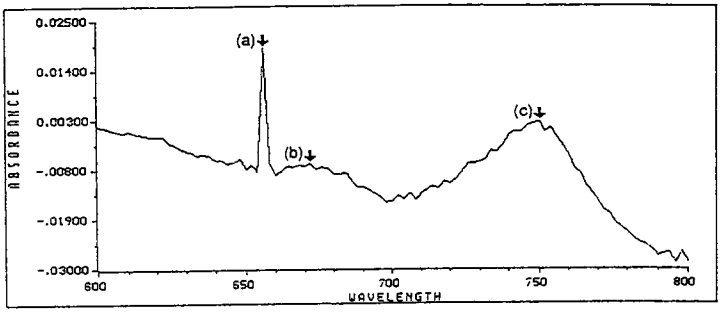

Figure 20. Absorbance of synthesized MB at 10 minutes after injecting a 10 mg/100 mL sulfide stock solution. Peak (a) is an instrumental artifact. Peak (b) is at 672 nm and -0.0067 AU and peak (c), at 750 nm and 0.0024 AU.

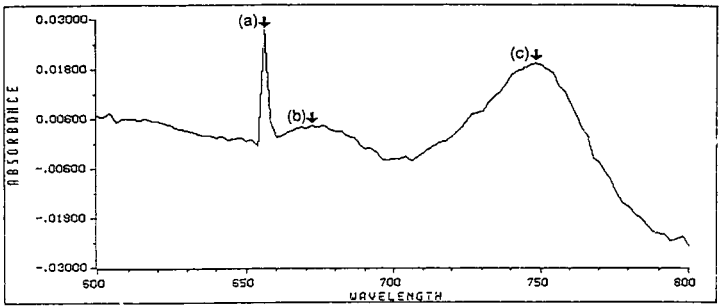

Figure 21. Absorbance of synthesized MB at 20 minutes after injection of a 10 mg/100 mL sulfide stock solution. Peak (a) is an instrumental artifact. Peak (b) is at 672 nm and 0.0043 AU and peak (c), at 748 nm and 0.0195 AU.

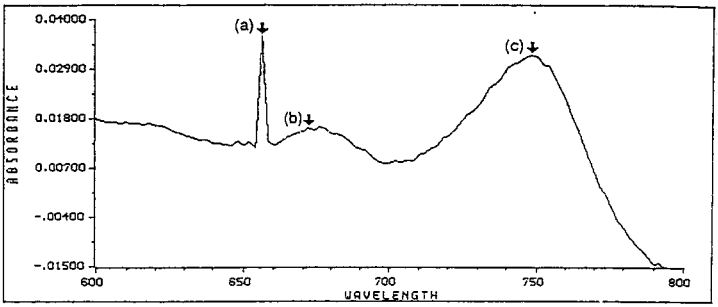

Figure 22. Absorbance of synthesized MB at 90 min after injecting a 10 mg/100 mL sulfide stock solution. Peak (a) is an instrumental artifact. Peak (b) is at 672 nm and 0.0159 AU; peak (c), at 748 nm and 0.0321 AU.

fluorescence intensity) of MB also differs with varying solution acidity. Figure 23 shows the fluorescence of MB in 2.00 M H_2SO_4; there is a broad peak with a maximum of 761 nm in addition to a scattering peak at ~ 700 nm. The lack of a fluorescence peak in this region in Figure 24 illustrates that the MB does not fluoresce strongly in 0.100 M H_2SO_4. Only a scatter peak is evident. Obviously, the quantum efficiency (the fraction of excited molecules that fluoresce) [2] of MB increases with decreasing pH. Both figures were obtained with conventional luminescence instrumentation using a slit width of 10 nm. The expansion factor (a scaling factor to adjust the ordinate display to the required value) for Figure 23 was 500; in Figure 24, 90.81. The signal shown in Figure 24 is larger than that in Figure 23.

Acidity Effects on DMPD. Evidently, the spectral characteristics of *N,N*-dimethyl-*p*-phenylenediamine (DMPD) vary with the acidity of the solution. Figure 25 is the absorbance spectrum of DMPD in 0.100 M H_2SO_4. There is a broad peak between 400 and 700 nm with a maximum absorbance of ~ 0.1 AU. Figure 26 presents the spectrum of this compound when in 2.00 M H_2SO_4; DMPD is not observed to absorb significantly between 400 and 700 nm when in a more acidic solution. The fluorescence of DMPD in 2.00 M and 0.100 M H_2SO_4 was also examined using an excitation wavelength of 280 nm. Figure 27 and 28 present the fluorescence spectrum for DMPD in 2.00 M H_2SO_4 and 0.100 M H_2SO_4, respectively. The fluorescence maximum for DMPD in 2.00 M H_2SO_4 is 354 nm; for DMPD in 0.100 M H_2SO_4, 384 nm. A conventional luminescence instrument was used with a slit width of 3 nm and a response factor of 4. The expansion factors are 19.75 in Figure 27 and 7.238 in Figure 28.

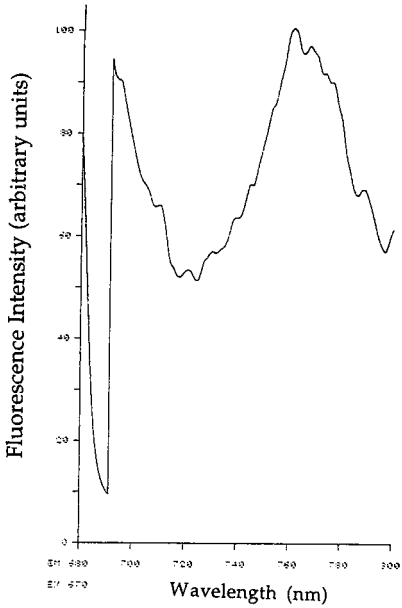

Figure 23. Fluorescence spectrum of MB in 2.00 M H_2SO_4. A broad peak results at a maximum of 761 nm in addition to a scatter peak at ~ 700 nm. Fluorescence is in relative fluorescence intensity units. Spectrum was obtained using a conventional luminescence instrument with a 10-nm slit width, and an expansion factor of 500.

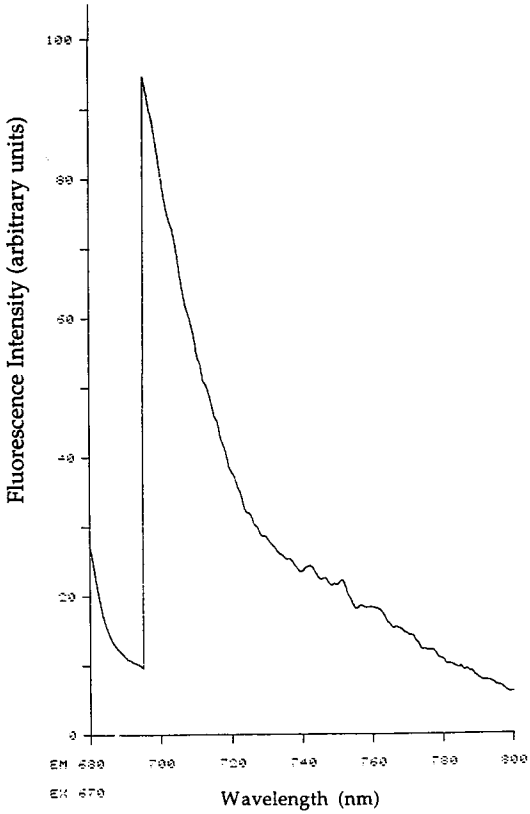

Figure 24. Fluorescence spectrum of MB in 0.100 M H_2SO_4. Only a scatter peak is evident. A conventional luminescence instrument was used with a slit width of 10 nm. The expansion factor is 90.81.

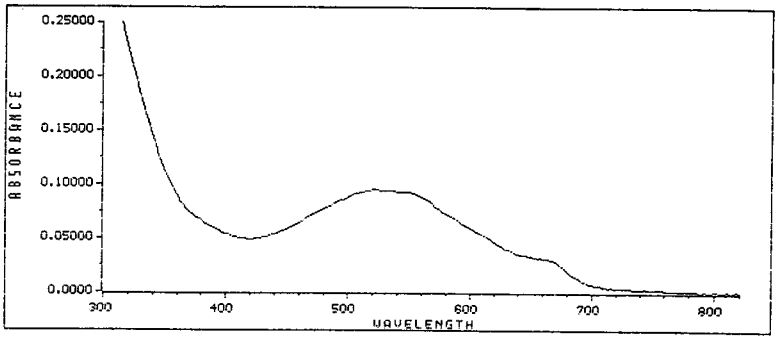

Figure 25. The absorption spectrum of DMPD in 0.100 M H_2SO_4. A broad peak is evident between 400 and 700 nm, with maximum absorbance of ~ 0.1 AU.

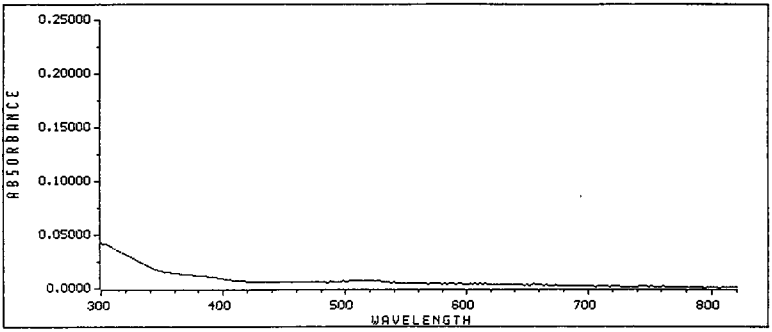

Figure 26. The absorption spectrum of DMPD in 2.00 M H_2SO_4. In comparison to Figure 25, DMPD does not illustrate a peak between 400 and 700 nm when in a more acidic solution.

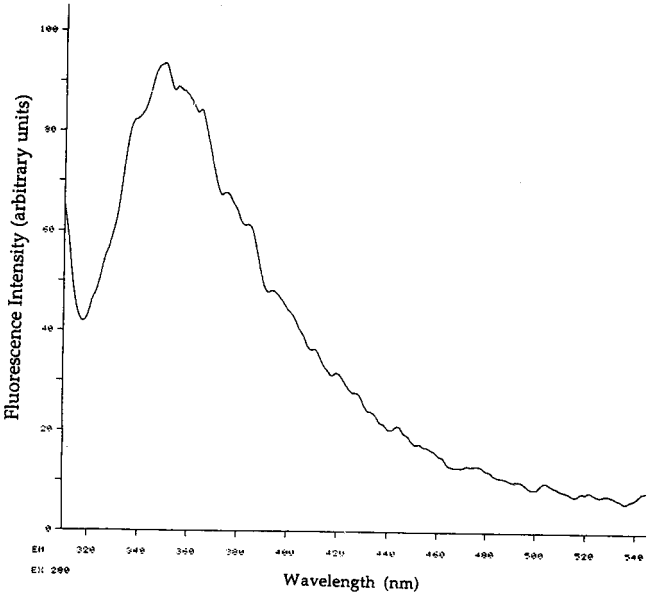

Figure 27. The fluorescence spectrum of DMPD in 2.00 M H_2SO_4. The excitation wavelength is 280 nm; the maximum fluorescence occurs at 354 nm. A conventional luminescence instrument was used with a slit width of 3 nm. The expansion factor is 19.75.

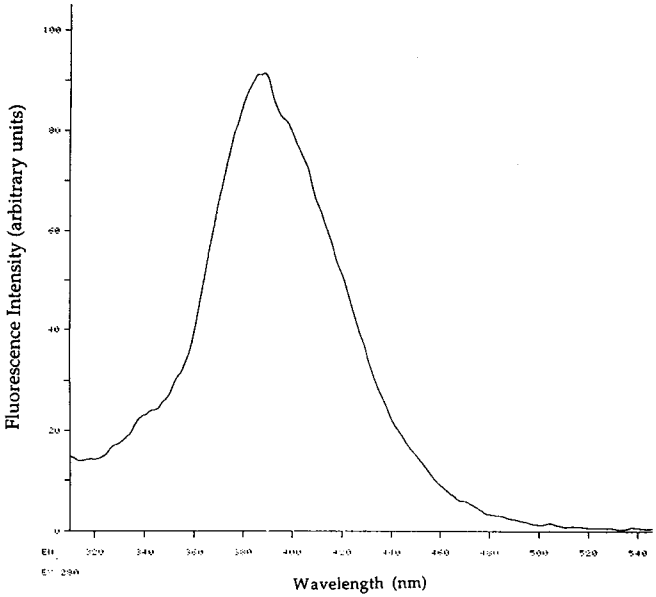

Figure 28. The fluorescence spectrum of DMPD in 0.100 M H_2SO_4. The excitation wavelength is 280 nm; the maximum fluorescence occurs at 384 nm. A conventional luminescence instrument was used with a slit width of 3 nm. The expansion factor is 7.238.

PART 3: THE DIODE-LASER-BASED DETECTOR WITH THE MB METHOD

Fluorescence 'Dips' in Response to MB. Currently, the fluorescence signal of the MB formed on-line or injected into an H_2O CS is indicated by an increase in negative voltage; we are observing fluorescence 'dips' rather than 'peaks' detected by the fluorescence photodiode. For example, when 1 mM MB is injected into an H_2O CS with similar lines, the result is a dip of 3.77 V. Injections of 1 mM MB with the MB Method reagent and carrier streams result in similar, if not larger, signals; concentrations of ~10^{-5} to ~10^{-6} M MB are quantifiable in both systems. All fluorescence data presented have been manipulated (by correcting for background, and in some cases, changing negative values to positive values) so the signal appears as a 'peak' rather than a 'dip'. The fluorescence of injected or on-line produced MB is in units of relative fluorescence intensity. This will be true for all fluorescence spectra in this report.

Laser Light Scatter. The amount of laser light scatter measured with water in the flow cell and detected by the fluorescence photodiode does not differ with or without use of the room lights. In addition, the amount of scatter detected does not differ with or without the use of the pump.

System Reproducibility and Its Response to Sulfide Injections of Varying Concentration. Fluorescence data obtained using the FI system and diode-laser-based detector are reproducible. Figure 29 presents the results of four replicate injections of 112 mg/L (4.66×10^{-4} M) sulfide; the DMPD CS is prepared in 2.00 M

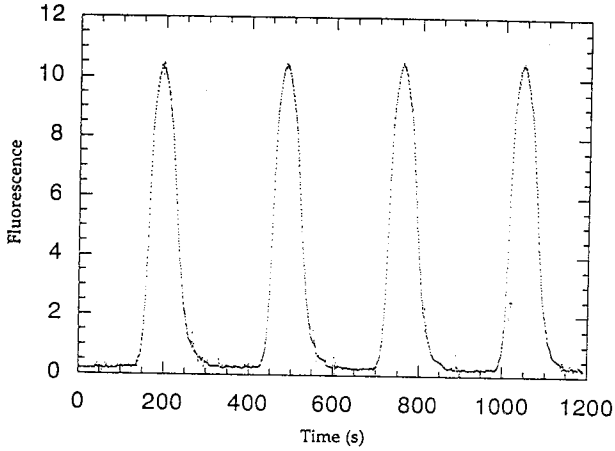

Figure 29. Reproducible fluorescence behavior in response to four sodium sulfide injections (112 mg/L) using DMPD in 2.00 M H_2SO_4. The peaks are indicative of on-line MB formation resulting from the reaction of S^{2-} with DMPD and Fe^{3+}.

H_2SO_4. The peaks are indicative of on-line MB formation. The fluorescence response to injections of sulfide of varying concentration (6.30 - 126 mg/L) with a DMPD CS containing 9.0 M H_2SO_4 is shown in Figure 30. Currently, the lowest quantified concentration of injected sulfide is 5.60 mg/L or 2.33×10^{-5} M.

The Linear Relationship between Fluorescence Response and Injected Sulfide Concentration. The fluorescence signal resulting from on-line formation of MB is linear with respect to the concentration of injected sulfide. Figures 31, 32, and 33 present the linear calibration curves for injected sulfide concentration (5.60 - 112 mg/L) with DMPD in 9.0 M, 4.5 M, and 2.0 M H_2SO_4 solutions, respectively. The slope is 16.2 (± 0.5), the intercept is -0.10 (± 0.06), and correlation coefficient (r^2) is 0.998 for the fluorescence response using 9.0 M H_2SO_4. Slope values of 23 (± 1) and 27 (± 2), intercepts of 0.0 (± 0.3) and -0.5 (± 0.3), and correlation coefficients equaling 0.990 and 0.988 result when employing DMPD in 4.5 M and 2.00 M H_2SO_4, respectively. More recently, sulfide was analyzed with a DMPD CS containing 0.100 M H_2SO_4; this is the lowest concentration of sulfuric acid we have employed. Figure 34 illustrates the linear relationship between fluorescence response to the on-line production of MB as a function of concentration. The slope is 7.4 (± 0.3), the intercept is -0.1 (± 0.1), and the correlation coefficient is 0.993.

The points plotted are the average values obtained. The average is representative of 2-5 multiple injections with one exception: in Figure 32, three of the six plotted points are not averaged because replicate measurements were not performed. Data have been taken at other concentrations, but due to a discovered systematic error in the pipette, these are omitted. No effort to

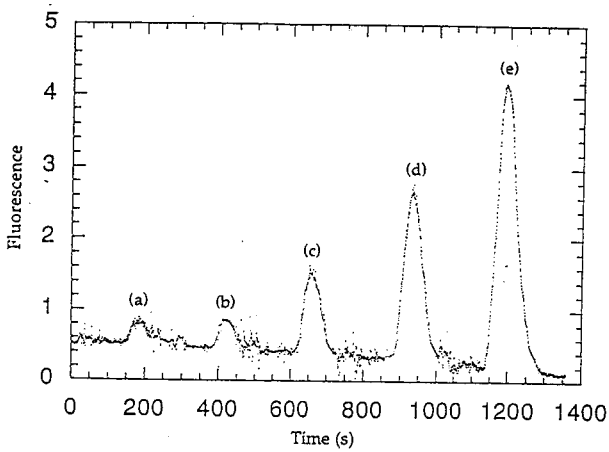

Figure 30. Fluorescence of on-line MB formation from sulfide injections of varying concentration using DMPD in 9.0 M H_2SO_4. The injected sulfide concentration at (a) is 6.30 mg/L; (b) 12.6 (mg/L); (c) 32.0 (mg/L); (d) 63.0 (mg/L); and (e) 126 (mg/L).

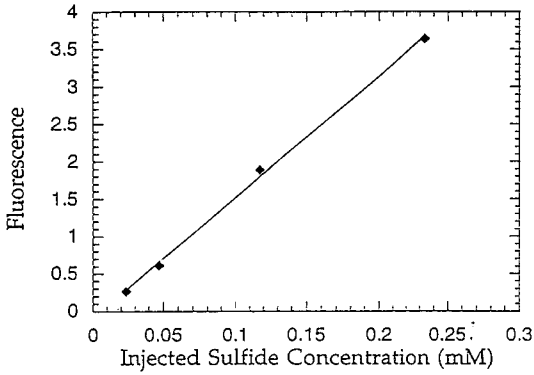

Figure 31. Fluorescence response to sulfide injections of varying concentration in a DMPD solution containing 9.0 M H_2SO_4. The line equation is as follows, where F is the fluorescence and $[S^{2-}]_{inj}$ is the concentration of injected sulfide: $F = -0.10\ (\pm 0.06) + 16.2\ (\pm 0.5)\ [S^{2-}]_{inj}$, $r^2 = 0.998$.

UN82 SPAZIANI, MICHELLE APPLICATIONS OF A DIODE-LASER, ETC.
S739a/1995 DEPT. OF CHEMISTRY HRS. 6/95 2/2

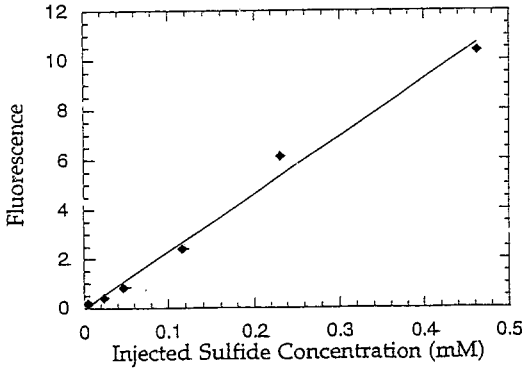

Figure 32. Fluorescence response to sulfide injections of varying concentration in a DMPD solution containing 4.5 M H_2SO_4. The line equation is as follows, where F is the fluorescence and $[S^{2-}]_{inj}$ is the concentration of injected sulfide: $[F] = 0.0\ (\pm 0.3) + 23\ (\pm 1)\ [S^{2-}]_{inj}$, $r^2 = 0.990$.

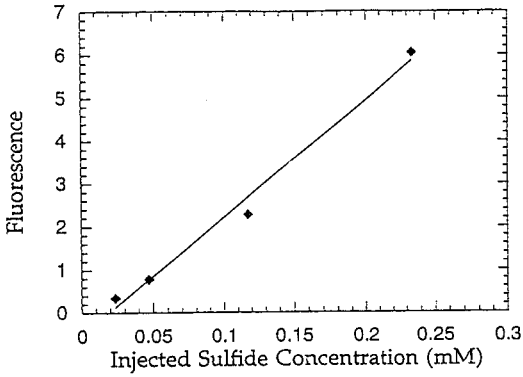

Figure 33. Fluorescence response to sulfide i jections of varying concentration in a DMPD solution containing 2.00 M H_2SO_4. The line equation is as follows, where F is the fluorescence and $[S^{2-}]_{inj}$ is the concentration of injected sulfide: $[F] = -0.5\ (\pm 0.3) + 27\ (\pm 2)\ [S^{2-}]_{inj}$, $r^2 = 0.988$.

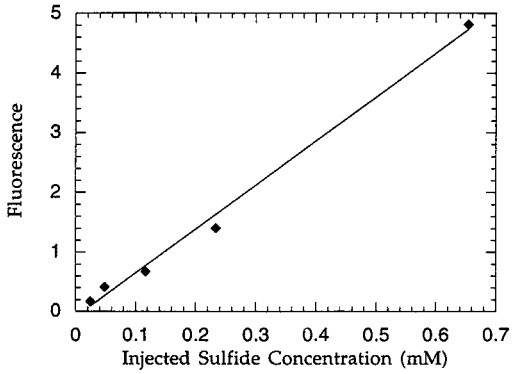

Figure 34. Fluorescence response to sulfide injections of varying concentration in a DMPD solution containing 0.100 M H_2SO_4. The line equation is as follows, where F is the fluorescence and $[S^{2-}]_{inj}$ is the concentration of injected sulfide: $[F] = -0.1\ (\pm 0.1) + 7.4\ (\pm 0.3)\ [S^{2-}]_{inj}$, $r^2 = 0.993$.

smooth the raw data has been made to date.

Limits of Detection. The limit of detection (LOD) for the fluorescence response to the on-line production of MB has been determined using 0.100 M, 2.00 M, 4.5 M, and 9.0 M H_2SO_4 in the DMPD CS {Table I}. Our LODs are three standard deviations (3 σ) above the mean background signal. These LODs can be compared to the extrapolated value reported by Kuban and coworkers [3]: 1 μg/L or 3.1×10^{-8} M.

Table I. Limits of detection (LODs) for sulfide, with or without a wastewater matrix, employing various concentrations of H_2SO_4 in the DMPD CS.

Concentration of acid used in DMPD CS (M)	wastewater used?	LOD (M injected sulfide)	LOD (mg/L injected sulfide)
9.0	No	2.4×10^{-6}	0.57
4.5	No	1.7×10^{-6}	0.41
2.00	No	1.4×10^{-6}	0.34
0.100	No	5.3×10^{-7}	0.13
2.00	Yes	1.9×10^{-6}	0.45
0.100	Yes	9.7×10^{-6}	2.3

The Response to Sulfide in a Simulated Wastewater Matrix. The fluorescence response to sulfide in an artificial matrix is reproducible (Figure 35). A 62 mg/L sulfide solution in simulated wastewater was injected in triplicate. This plot can be compared to the fluorescence response of a 56 mg/L sulfide solution without a wastewater matrix in terms of both reproducibility and size of fluorescence peaks (Figure 36). Table II (page 65) presents the average height of the fluorescence signal detected when using an approximate 30 mg/L sulfide solution either in water or a simulated wastewater matrix. All averages are based on 3-4 replicate measurements except for the determination of sulfide (without the wastewater matrix) using 4.5 M H_2SO_4 in the DMPD CS; this finding is based on only one measurement.

The fluorescence signal resulting from on-line formation of MB is linear with respect to the concentration of injected sulfide in an artificial wastewater matrix. Again, the averages of the data points have been plotted, and no effort to smooth the data has been made.

The on-line fluorescence response to varying concentrations of sulfide prepared in an artificial matrix is illustrated in Figures 37 and 38. A DMPD CS containing 2.00 M H_2SO_4 or 0.100 M H_2SO_4 was used in Figures 37 and 38, respectively. In the former, the slope is 20.6 (± 0.2), the intercept is 0.09 (± 0.06), and the correlation coefficient is 1.00. When employing a DMPD CS in 0.100 M H_2SO_4, the intercept is 0.0 (± 0.1), the slope is 4.0 (± 0.4), and r^2 is 0.990; however, this line equation is based on only three plotted points. The LODs for sulfide in the complex matrix using 2.00 M or 0.100 M H_2SO_4 are comparable to those determined for sulfide alone (Table I).

Table II. Average height of the fluorescence signal when using an approximate 30 mg/L sulfide solution either in water or a simulated wastewater matrix.

Concentration of acid used in DMPD CS (M)	wastewater used?	Concentration of injected sulfide (M)	Average size of fluorescence peak (V)
9.0	No	1.17×10^{-4}	1.19
4.5	No	1.16×10^{-4}	2.42
2.00	No	1.17×10^{-4}	2.28
0.100	No	1.17×10^{-4}	0.68
2.00	Yes	1.29×10^{-4}	2.84
0.100	Yes	1.29×10^{-4}	0.44

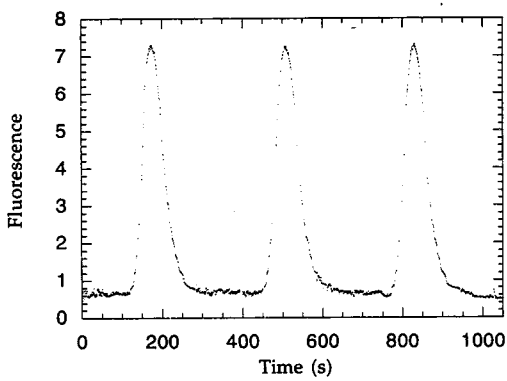

Figure 35. Reproducible fluorescence behavior to replicate injections of a 62 mg/L sulfide solution, which is in simulated wastewater, into C1 {Figure 16}. The DMPD CS contains 2.00 M H_2SO_4.

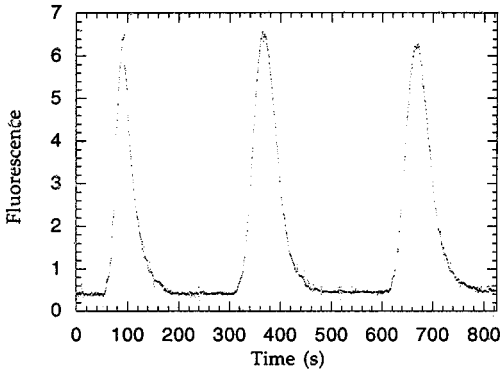

Figure 36. Reproducible fluorescence peaks in response to sulfide injections (56 mg/L) without wastewater. The DMPD CS contains 2.00 M H_2SO_4.

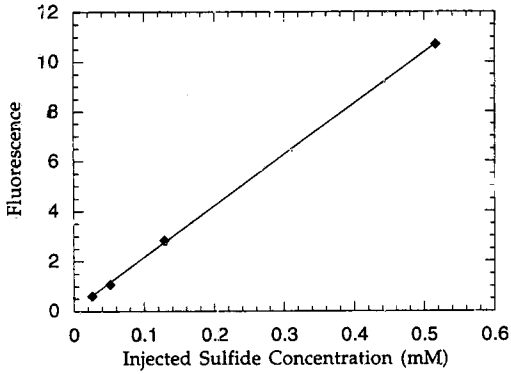

Figure 37. The on-line fluorescence response to varying concentrations of sulfide prepared in an artificial matrix. The DMPD CS contains 2.00 M H_2SO_4. The line equation is as follows, where F is the fluorescence and $[S^{2-}]_{inj}$ is the concentration of injected sulfide: F = 0.09 (± 0.06) + 20.6 (± 0.2) $[S^{2-}]_{inj}$, r^2 = 1.00.

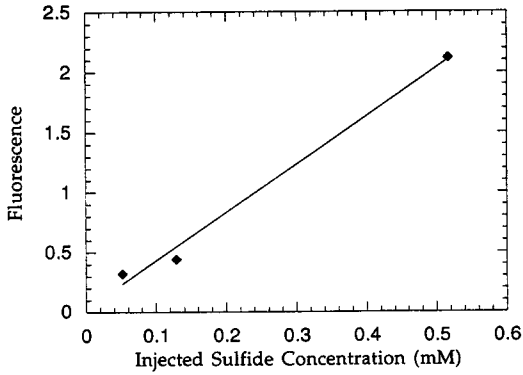

Figure 38. The on-line fluorescence response to varying concentrations of sulfide prepared in an artificial matrix. The DMPD CS contains 0.100 M H_2SO_4. The line equation is as follows, where F is the fluorescence and $[S^{2-}]_{inj}$ is the concentration of injected sulfide: F = 0.0 (± 0.1) + 4.0 (± 0.4) $[S^{2-}]_{inj}$, r^2 = 0.990.

Literature Cited

[1] Davis, J.L.; Senior Thesis, Union College, 1993.

[2] Harris, D.C.; *Quantitative Chemical Analysis*, 3rd ed.; W.H. Freeman and Company: New York, 1991; 570.

[3] Kuban, V.; Dasgupta, P.K.; Marx, J.N.; *Anal. Chem.* **1992**, *64*, 36-43.

Chapter 4

Discussion

We have shown that with a diode-laser-based detector and fluorescence detection, the determination of sulfide using the Methylene blue (MB) Method can be performed under less corrosive conditions than reported in the literature [1]. Because of the disadvantages of performing routine analysis with strongly acidic solutions, we have examined the MB method using less acidic solutions, i.e. 4.5 M, 2.00 M, and 0.100 M H_2SO_4. The data presented here have been obtained while working under conditions approximating those in the literature [1]. No attempt at further optimization of reaction rates or other conditions was made.

Our flow rates are lower than those stated in the literature [1], where C1 flowed at 0.6 mL/min, while C2 and C3 flowed at 0.3 mL/min {Figure 16}. Obviously, under our conditions the reaction proceeds at a slower rate, hence allowing a greater time for on-line reaction and a larger fluorescence signal at the detector.

The dispersion coefficient (D) has been determined via diode-laser fluorescence and diode array absorbance. D is 10.4 and 8.30 for fluorescence and absorbance detection, respectively. This indicates that the concentration of injected sulfide is approximately one order of magnitude lower when at the detector.

Originally, we anticipated a larger dispersion due to the extensive length of tubing used and the slow flow rates. Others [2] with a similar system reported a dilution factor of ~55, which seems more reasonable based on these factors. However, D of ~10 is still a large dispersion, therefore explaining the extensive

band-broadening of the on-line MB formation peak at the detector.

The fluorescence response to the on-line production of MB is reproducible {Figure 29}. In addition, the fluorescence response to varying concentrations of injected S^{2-} using *N,N*-dimethyl-*p*-phenylenediamine (DMPD) containing 9.0 M H_2SO_4 illustrates that the fluorescence of the on-line formed MB increases with increasing sulfide concentration {Figure 30}. Put simply, more MB is produced with increasing sulfide concentration, hence increasing the amount of fluorescence detected.

The linear calibration curves show that the on-line reaction can be performed using 9.0 M H_2SO_4 as recommended in the literature [1], and sulfuric acid of lower concentration. In terms of the size of the fluorescence peak at the detector, our best results are evident in Figure 33; the overall fluorescence response to varying concentrations of injected $Na_2S_{(aq)}$ using a DMPD carrier containing 2.00 M H_2SO_4 was observed to be greater than twice that obtained when using DMPD in 9.0 M H_2SO_4. Table II lists the size of the fluorescence peak for 1.17×10^{-4} M injected sulfide as 2.28 V compared to 1.19 V when using 9.0 M H_2SO_4 at the same concentration of injected sulfide. At this particular concentration, the difference is ~ 1.91 V.

The explanation for this phenomenon, the increased fluorescence of on-line produced MB when in 2.00 M H_2SO_4, is two-fold. First, the fluorescence detection of the on-line formation of MB is more sensitive when using 2.00 M H_2SO_4 because the molar absorptivity at the wavelength of the laser and the observed fluorescence intensity are greater. Secondly, after final mixing in the manifold, the reagent stream has been diluted to a pH at which the MB is almost

completely in the MB^+ form {Figure 10}. At this pH, the MB formed exhibits the largest fluorescence signal because the absorbance maximum (664 nm) is almost exactly the excitation wavelength of the diode laser (670 nm).

Currently, the lowest concentration of sulfuric acid employed is 0.100 M H_2SO_4 in the DMPD carrier stream (CS). The fluorescence response to on-line MB formation using this solution is linear, as expected {Figure 34}. The smaller fluorescence signals obtained, however, were unexpected. Initially, we hypothesized that the fluorescence of the on-line formed MB would increase as the concentration of sulfuric acid decreased. This theory was based on the argument presented previously.

Unlike the other colorless and clear DMPD solutions, DMPD containing 0.100 M H_2SO_4 is purple. Furthermore, the strength of the purple color evolves with time. The fluorescence of the DMPD solution in 2.00 M H_2SO_4 does not differ drastically from that in 0.100 M H_2SO_4 {Figures 27, 28}; the purple DMPD solution, therefore, is not to blame for the smaller fluorescence signals because the DMPD solution does not fluoresce in the same part of the UV-Vis spectral region in which MB emits. However, the absorbance difference between these solutions may be responsible for the change in fluorescence signal size. The absorbance of DMPD in 0.100 M H_2SO_4 {Figure 25} at 670 nm is significant, whereas the absorbance of DMPD in 2.00 M H_2SO_4 is insignificant {Figure 26}. We would actually expect that the DMPD absorption in this region would prevent some of the fluorescence collection at the detector. Perhaps the DMPD forms an intermediate when in 0.100 M H_2SO_4, which would account for the purple color. If DMPD is in an intermediate form, there is less DMPD to react with the other reagents and sulfide, hence less MB formed on-line and less

fluorescence is observed at the detector.

Ironically, the solution that inhibits some fluorescence at the detector brings about our lowest limit of detection (LOD). We have achieved the best results employing a DMPD solution containing 0.100 M H_2SO_4; our LOD is 5.3 x 10^{-7} M injected sulfide {Table I}. This solution is substantially less acidic than the 9.0 M H_2SO_4 reported in the literature, and subsequently, a more practical reagent stream for routine analysis.

Data obtained when using sulfide in a simulated wastewater matrix shows that the fluorescence response to sulfide is linear {Figures 37, 38}. In fact, the size of the MB fluorescence peaks is relatively similar to those without an artificial matrix {Table II}. The LOD for injected sulfide in a simulated wastewater matrix with a DMPD CS containing 2.00 M H_2SO_4 is very similar to that without the matrix {Table I}. Unfortunately, that resulting from use of a DMPD CS in 0.100 M H_2SO_4 is ~ 0.05 M higher than the LOD value obtained without wastewater. This LOD determination, however, has been obtained based on a calibration curve of only three points {Figure 38}. It is expected that the LOD will decrease after more data has been collected.

If a sulfide sample in the simulated wastewater is treated as an unknown, the concentration is, for the most part, similar according to the particular calibration curve of fluorescence vs. injected sulfide concentration. For example, when a 5.16 x 10^{-4} M sulfide in the matrix is injected into the flow injection (FI) system employing a DMPD CS in 2.00 M H_2SO_4 a 10.8 V fluorescence signal results. Using Microsoft Excel's Linear Least Squares (LLS), the calculated concentration of this solution is 4.1 (± 0.2) x 10^{-4} M S^{2-}. Table III

lists other calculated concentrations and their errors for all injected sulfide solutions in a wastewater matrix at 2.00 M and 0.100 M H_2SO_4. The error is attributed partly to the matrix and partly to taking measurements on different days. Generally, the fluorescence response to MB produced on-line is unaffected by the artificial wastewater matrix.

Table III. Calculated concentrations by LLS of injected sulfide solutions in a simulated wastewater matrix.

Concentration of acid DMPD CS (M)	Actual concentration of injected sulfide (M)	Calculated concentration of injected sulfide (M)
2.00	5.16×10^{-4}	$4.1 (\pm 0.2) \times 10^{-4}$
	1.29×10^{-4}	$1.2 (\pm 0.1) \times 10^{-4}$
	5.16×10^{-5}	$5 (\pm 1) \times 10^{-5}$
	2.58×10^{-5}	$4 (\pm 2) \times 10^{-5}$
0.100	5.16×10^{-4}	$3.0 (\pm .3) \times 10^{-4}$
	1.29×10^{-4}	$0.7 (\pm .3) \times 10^{-4}$
	5.16×10^{-5}	$5 (\pm 3) \times 10^{-5}$

Presently, our LODs are slightly higher than that reported by Kuban and coworkers [1] using a DMPD reagent line in 9.0 M sulfuric acid. The authors [1] report an extrapolated LOD of 1 μg/L S^{2-}, or 3.1×10^{-8} M S^{2-}, over the

concentration range of 0-90 μg/L. However, they do not specify whether this value is representative of the concentration of injected sulfide or the concentration of the MB at the detector. Undoubtedly, there is a large difference.

If their LOD [1] is the concentration of injected sulfide at the detector, and we assume their D is at least 10, then they claim they can detect 3.1×10^{-9} M MB at the detector. (There is the possibility that Kuban and coauthors had a smaller dispersion due to a smaller sample injection of only 20 μL. In addition, because they used much faster flow rates, their value for D may have also been larger.) Measuring the absorbance of this concentration is virtually impossible using a conventional UV-Vis detector. Figure 39 illustrates the steady-state absorbance spectrum of 0.01 μM MB in water (using a newer diode array spectrophotometer model than Kuban and coworkers [1]). Comparing this spectrum to 1 μM MB in Figure 11, the broad peak in Figure 39 is in the same region as the maximum peak at 664 nm in Figure 11. However, the maximum absorbances are not comparable; the absorbance of the 0.01 μM MB is ~ 0.001 absorbance units, which is not similar to the absorbance of 1 μM MB (~0.08 AU). Obviously, it would be difficult to quantitatively or qualitatively study MB from the steady-state absorbance spectrum of 0.01 μM MB in Figure 39.

In addition, Kuban and coworkers [1] used an absorbance cell of path length 3 mm, which is three times smaller than that used in our absorption data. With this in mind, and while assuming that the literature LOD represents the concentration of injected sulfide, the authors [1] state that the 0.01 μM MB solution is detectable with a signal that is less than one-third the signal seen in Figure 11 because of dispersion. This is unlikely.

We can conclude that Kuban and coworkers are not reporting a LOD for

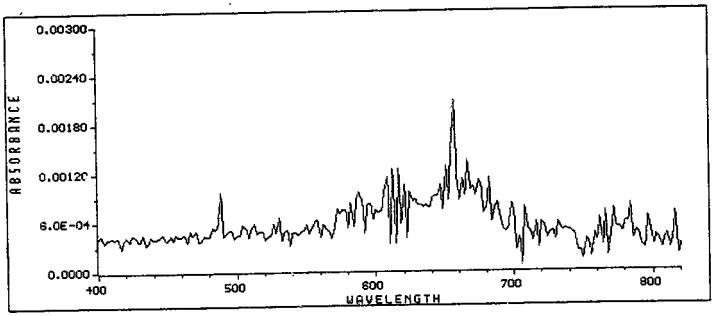

Figure 39. Absorption spectrum of 0.01 μM MB in water.

the concentration of injected sulfide but rather for the concentration of MB at the detector. This being said, our LOD values are similar to that given in the literature [1]. However, they are much higher than anticipated using a fluorescence-based detector.

The higher LODs result from several noise limitations. First, the slow reaction rates require flow rates at levels where fluctuations in the flow of the carrier and reagent stream affect the data observed. These fluctuations could be avoided by increasing the flow rates, yet the amount of MB formed on-line would then decrease, resulting in a smaller fluorescence signal. Secondly, the mechanical instability of the flow cell (FC) has caused an increase in the amount of noise produced. Thirdly, the current-to-voltage conversion circuitry causes greater noise. Modifications of the flow rates, more stable positioning of the flow cell, and improved current-to-voltage circuit design will allow for a lower LOD.

There are several discrepancies between the results presented here and those found in the Kuban and coworkers report [1]. Contrary to the literature [1], we have shown that with diode-laser-based fluorescence detection, the MB Method works well using lower concentrations of sulfuric acid in the DMPD CS. Secondly, highly concentrated sulfuric acid in the solution is not necessary to achieve greater reaction rates as Kuban et al. report; we qualitatively observed a similar rate of reaction employing sulfuric acid of varying concentrations. Thirdly, a highly concentrated sulfuric acid in the DMPD CS is unnecessary to provide great immunity at 670 nm from indigenous material present in an artificial wastewater matrix; data obtained when using 2.00 M or 0.100 M H_2SO_4 in the DMPD CS and sulfide in a simulated wastewater matrix are similar to those obtained without use of a wastewater. In addition, we did not observe a

substantial heat of hydration in the RC resulting from the strongly acidic (9.0M, 4.5 M, 2.00 M) H_2SO_4 solutions {Figure 16}. Lastly and most importantly, our data show the fluorescence of the on-line produced MB is greater employing 2.00 M H_2SO_4 rather than 9.0 M H_2SO_4. Kuban and coworkers were detecting farther in the red (745 nm) and may have needed a highly acidic solution to ensure that all the MB was in the proper form (MBH^{2+}), rather than to facilitate the reaction. Therefore, we conclude that the optimized conditions reported by Kuban and coauthors for absorbance-based detection a 745 nm are not optimized conditions for fluorescence detection.

Literature Cited

[1] Kuban, V.; Dasgupta, P.K.; Marx, J.N.; *Anal. Chem.* **1992,** *64,* 36-43.

[2] Lei, W.; Dasgupta, P.K.; *Anal. Chim. Acta* **1989,** *226,* 165-170.

Chapter 5

Future Research

Future work will include analyzing $Na_2S_{(aq)}$ with *N,N*-dimethyl-*p*-phenylenediamine (DMPD) solutions of even lower H_2SO_4 concentrations. Further optimization of the Methylene Blue (MB) Method and subsequent improvement of the detection limits using the diode-laser-based detector and flow injection (FI) apparatus will be performed. More specifically, we anticipate studying the reaction kinetics and the product yield as affected by the concentration of the reactants, the ratio of Fe^{3+} to DMPD, the order of reagent addition, the reaction times allowed for the individual steps, and the form in which Fe^{3+} is added [1]. We also hope to quantitatively prove that the reaction kinetics are independent of the reaction acidity, unlike the product yield, which has been shown in this report.

To further illustrate the applicability of the MB Method with the diode-laser detector, we intend to analyze sulfide samples in an artificial wastewater matrix [1] using lower concentrations of H_2SO_4. The fluorescence response to sulfide is expected to be unaffected by the synthetic wastewater at any concentration of sulfuric acid because the reaction is specific to sulfide. In addition, improvement of the limit of detection (LOD) specifically using 0.100 M sulfuric acid and sulfide in a wastewater matrix is necessary.

Finally, the light collection of the fluorescence detector will be optimized; no focusing optics are used at present. Clearly, increasing the amount of incident light on the detector will result in a larger signal and a lower LOD.

Literature Cited

[1] Kuban, V.; Dasgupta, P.K.; Marx, J.N.; *Anal. Chem.* **1992**, *64*, 36-43.